0026-895X/07/7205-1157–1170$20.00
MOLECULAR PHARMACOLOGY
Vol. 72, No. 5

34769/3268047
*Mol Pharmacol* 72:1157–1170, 2007
*Printed in U.S.A.*

# Regulation of D1 Dopamine Receptor Trafficking and Signaling by Caveolin-1

Michael M. C. Kong, Ahmed Hasbi, Michael Mattocks, Theresa Fan, Brian F. O'Dowd, and Susan R. George

*Departments of Pharmacology (M.M.C.K., A.H., M.M., T.F., B.F.O., S.R.G.) and Medicine (S.R.G.), University of Toronto, Toronto, Ontario, Canada; and Centre for Addiction and Mental Health, Toronto, Ontario, Canada (T.F., B.F.O., S.R.G.)*

Received February 4, 2007; accepted August 15, 2007

## ABSTRACT

There is accumulating evidence that G protein-coupled receptor signaling is regulated by localization in lipid raft microdomains. In this report, we determined that the D1 dopamine receptor (D1R) is localized in caveolae, a subset of lipid rafts, by sucrose gradient fractionation and confocal microscopy. Through coimmunoprecipitation and bioluminescence resonance energy transfer assays, we demonstrated that this localization was mediated by an interaction between caveolin-1 and D1R in COS-7 cells and an isoform-selective interaction between D1R and caveolin-1$\alpha$ in rat brain. We determined that the D1R interaction with caveolin-1 required a putative caveolin binding motif identified in transmembrane domain 7. Agonist stimulation of D1R caused translocation of D1R into caveolin-1-enriched sucrose fractions, which was determined to be a result of D1R endocytosis through caveolae. This was found to be protein kinase A-independent and a kinetically slower process than clathrin-mediated endocytosis. Site-directed mutagenesis of the caveolin binding motif at amino acids Phe313 and Trp318 significantly attenuated caveolar endocytosis of D1R. We also found that these caveolin binding mutants had a diminished capacity to stimulate cAMP production, which was determined to be due to constitutive desensitization of these receptors. In contrast, we found that D1Rs had an enhanced ability to maximally generate cAMP in chemically induced caveolae-disrupted cells. Taken together, these data suggest that caveolae has an important role in regulating D1R turnover and signaling in brain.

Caveolae have a well defined role in mediating the activity of a number of signal transduction pathways, including those involving receptor tyrosine kinases (Yamamoto et al., 1998) and multichain immune recognition receptors (Dykstra et al., 2001). There is emerging evidence that G protein-coupled receptor (GPCR) function is also modulated by localization in caveolae, because a wide array of GPCR-signaling molecules, including G proteins, regulator of G protein signaling proteins, and protein kinases, have been reported to compartmentalize in these microdomains (Allen et al., 2007). The caveolar localization of GPCRs has been reported to have various functional consequences, with roles in agonist signaling, internalization, and the activation of various effector pathways (Igarashi and Michel, 2000; Rybin et al., 2000; Bhatnagar et al., 2004).

Caveolae represent a subtype of lipid rafts that exist as morphologically distinct invaginations at the plasma membrane. These lipid-enriched entities move laterally on the cell surface while allowing the exchange of proteins and lipids between the raft domain and the surrounding liquid-disordered phospholipid environment (Rajendran and Simons, 2005). This dynamic regulation is thought to facilitate the formation of cell surface signaling platforms for the integration of various signaling molecules, thus ensuring specificity and efficiency in signal transduction processes. The caveolin proteins are unique to caveolae, and they serve a dual role in

This work was supported by the National Institute on Drug Abuse and the Canadian Institutes of Health Research. S.R.G is a Canada Research Chair in Molecular Neuroscience.
Article, publication date, and citation information can be found at http://molpharm.aspetjournals.org.
doi:10.1124/mol.107.034769.

**ABBREVIATIONS:** GPCR, G protein-coupled receptor; D1R, D1 dopamine receptor; H89, *N*-[2-(4-bromocinnamylamino)ethyl]-5-isoquinoline; TM, transmembrane; SCH23390, *R*-(+)-7-chloro-8-hydroxy-3-methyl-1-phenyl-2,3,4,5-tetrahydro-1*H*-3-benzazepine; GTP$\gamma$S, guanosine 5′-*O*-(3-thio)triphosphate; GFP, green fluorescent protein; mRFP, monomeric red fluorescent protein; eGFP, enhanced green fluorescent protein; Rluc, *Renilla reniformis* luciferase; GRK, G protein receptor kinase; HEK, human embryonic kidney; PAGE, polyacrylamide gel electrophoresis; ARF, ADP ribosylation factor; HA, hemagglutinin; HRP, horseradish peroxidase; PBS, phosphate-buffered saline; CHAPS, 3-[(3-cholamidopropyl)dimethylammonio]propanesulfonate; O/N, overnight; RT, room temperature; SKF 81297, ($\pm$)-6-chloro-7,8-dihydroxy-1-phenyl-2,3,4,5-tetrahydro-1*H*-3-benzazepine hydrobromide; BRET, bioluminescence resonance energy transfer; m$\beta$CD, methyl-$\beta$-cyclodextrin; PKA, protein kinase A; CBM, caveolin binding motif.

maintaining the structural integrity of caveolae and by acting as a scaffolding protein that binds to a battery of receptors, signaling molecules, and adapter proteins (Williams and Lisanti, 2004). There are three caveolin isoforms, each of which can serve as biochemical markers for the identification of caveolae; caveolin-1 is the most ubiquitously expressed, because it is found in tissues including the lung, heart, and brain, whereas caveolin-3 is specific to muscle. The expression of caveolin-1 in brain has been shown in neuronal cells such as hippocampal and dorsal root ganglion neurons (Galbiati et al., 1998; Bu et al., 2003) as well as glial cells such as astrocytes and oligodendrocytes (Cameron et al., 1997).

Despite the presence of caveolin-1 in brain, there is little known about how this ubiquitous protein modulates the function of those GPCRs that are involved in critical aspects of brain function. The D1 dopamine receptor (D1R) is the most abundant dopamine receptor subtype in the brain, with an expression profile that covers various regions, including the striatum, nucleus accumbens, and hippocampus. There is also evidence for its expression in glial cells, particularly astrocytes, from striatum and basal ganglia (Zanassi et al., 1999; Miyazaki et al., 2004). In the brain, D1R participates in the modulation of various neural processes, including learning, memory, reward, and locomotor activity. The D1R couples to $G_s/G_{olf}$ to activate the adenylyl cyclase effector pathway, which, in turn, modulates intracellular levels of cAMP. Many components of this signaling pathway, such as $G_s\alpha$ and specific adenylyl cyclase isoforms, compartmentalize in caveolae, suggesting that receptors such as D1R that are associated with this signaling cascade might also localize in these microdomains. The ability of such signaling molecules to localize in caveolae has been proposed to be mediated by a direct interaction between the scaffolding domain of caveolin-1 and a putative caveolin binding motif found in most caveolae-associated proteins (Couet et al., 1997). This binding motif is characterized by the amino acid sequence $\phi X\phi XXXX\phi$, $\phi XXXX\phi XX\phi$, or $\phi X\phi XXXX\phi XX\phi$ [where X is any amino acid and $\phi$ is one of the aromatic amino acids (Trp, Phe, or Tyr)]. We found that D1R contains a caveolin binding motif in the proximal region of the seventh transmembrane (TM) domain, thus implying a role for caveolin in D1R function.

In this study, we show that D1R is localized in low-density caveolin-enriched membrane domains; this was due to a direct interaction with endogenously expressed caveolin-1 in heterologously expressed cells and in rat brain. We also report that agonist-mediated D1R endocytosis occurred through a caveolin-dependent pathway that had internalization kinetics distinct from clathrin-mediated endocytosis. We found that this novel mode of D1R internalization was dependent on the integrity of caveolae, because disruption of caveolae strongly reduced agonist-mediated receptor sequestration. This was corroborated by studies showing that mutation of the caveolin binding motif in D1R also attenuated receptor internalization. We also report that the disruption of caveolae had significant effects on G-protein coupling and agonist-induced cAMP production of D1R. These results suggest that D1R function is profoundly regulated by caveolin-1 in regions where both proteins may coexist, such as glial cells and hippocampal neurons of the brain.





## Materials and Methods

**Chemicals.** Concanavalin A was purchased from Calbiochem (San Diego, CA). Filipin, methyl-$\beta$-cyclodextrin, and H89 were purchased from Sigma-Aldrich (St. Louis, MO). $[^3H]$SCH23390 (85 Ci/mmol) and $[^{35}S]$GTP$\gamma$S (1250 Ci/mmol) were purchased from PerkinElmer Life and Analytical Sciences (Boston, MA).

**DNA Constructs and Site-Directed Mutagenesis.** We used the full-length D1 dopamine receptor cDNA that was cloned into the mammalian expression vector pcDNA3.1 (Invitrogen, Carlsbad, CA) as a template for site-directed mutagenesis studies. The mutant dopamine D1 constructs F313A, W318A, W321A, and FWW/A and mutant caveolin-1 P132L were generated using the QuikChange site-directed mutagenesis kit (Stratagene, La Jolla, CA). The wild-type cMyc caveolin-1 was a kind gift provided by Dr. Bryan Roth (University of North Carolina, Chapel Hill, NC). The dominant-negative G protein receptor kinase (GRK)2-K220R was a kind gift from Dr. Jeffrey Benovic (Thomas Jefferson University, Philadelphia, PA). The caveolin-1-GFP and D1R-GFP constructs were designed by cloning caveolin-1 and D1R, respectively, into pEGFP-N1 (BD Biosciences, San Jose, CA) in frame with GFP at the carboxyl tail. The D1R-mRFP construct was generated in a similar manner by isolating mRFP (in pRSETb vector) by polymerase chain reaction and replacing GFP from the pEGFP-N1 vector with mRFP. The D1R-Rluc construct was created by replacing the eGFP from D1R-GFP with Rluc.

**Cell Culture and DNA Transfection.** COS-7 and HEK293t cells were maintained as monolayer cultures at 37°C in $\alpha$-minimum essential medium (University of Toronto, Toronto, ON, Canada) or advanced minimum essential medium (Invitrogen), respectively, supplemented with 10% fetal bovine serum, antimycotic and antibiotic. Cells were grown to 80% confluence before being transfected using Lipofectamine 2000 (Invitrogen). For coexpression experiments, the total amount of cDNA transfected under control conditions was kept constant by the addition of a compensating amount of pcDNA3. Transfected cells were grown for 48 h before harvesting for all functional assays.

**Detergent-Free Sucrose Gradient Fractionation.** Caveolae-enriched fractions were prepared by separating whole cell lysates on a discontinuous sucrose gradient column by ultracentrifugation. Each gradient column was prepared with transfected COS-7 cells from three 100-mm dishes or from 3 mg of whole rat brain lysate. Lysates were scraped into 2 ml of buffer containing 500 mM sodium carbonate, pH 11, and sonicated before bringing to 45% sucrose (w/v) by adding 2 ml of 90% sucrose, prepared in 25 mM 2-[*N*-morpholino]ethanesulfonic acid and 150 mM NaCl. The resulting cell suspension was placed at the bottom of a 12-ml ultracentrifuge tube. A discontinuous gradient was prepared by sequentially layering 4 ml of 35% sucrose and 5% sucrose (prepared in 25 mM 2-[*N*-morpholino]ethanesulfonic acid and 150 mM NaCl and carbonate buffer) on top of the 45% sucrose bed. After centrifugation at 35,000 rpm for 20 h at 4°C, 1-ml fractions were collected from the top of each gradient, and they were subjected to 20% trichloroacetic acid precipitation. Protein pellets were subsequently washed with acetone and resuspended in a 1:1 solution of 5:2 lysis buffer (5 mM Tris-HCl and 2 mM EDTA) and Laemmli buffer. An equal volume of each fraction was separated on SDS-PAGE and immunoblotted with the antibodies indicated. The antibodies used were anti-$Na^+/K^+$ ATPase (Developmental Studies Hybridoma Bank, University of Iowa, Iowa City, IA), mouse anti-caveolin-1 (BD Biosciences), anti-HA-horseradish peroxidase (HRP) (Roche, Penzburg, Germany), rabbit anti-$G_s\alpha$ (Santa Cruz Biotechnology, Inc., Santa Cruz, CA), goat anti-clathrin heavy chain (Santa Cruz Biotechnology, Inc.), mouse anti-ARF6 (Santa Cruz Biotechnology, Inc.), and rat anti-D1R (Sigma-Aldrich). The protein bands were scanned by densitometric analysis, and relative intensities were quantified using National Institutes of Health Image J software version 1.33 (http://rsb.info.nih.gov/ij/).

**Coimmunoprecipitation.** Transfected COS-7 cells were washed in PBS and scraped into homogenization buffer consisting of 50 mM Tris-HCl, 150 mM NaCl, 1 mM EDTA, 2.5 mM $MgCl_2$, and protease inhibitors. Cells were harvested by disruption with a Polytron homogenizer (Brinkmann, Westbury, NY) and centrifuged at 1000*g* for 10 min. Then, 2 mg of supernatant was collected and solubilized by addition of Nonidet P-40 to a final concentration of 1% (v/v) for 2 h at 4°C. Samples were centrifuged at 20,000*g* for 20 min, and the supernatant was collected and recentrifuged again. After preclearing for 20 min with 20 $\mu$l of protein G agarose beads (Sigma-Aldrich), the lysates were incubated overnight with 5 $\mu$g of rabbit polyclonal anti-HA (BD Biosciences) or mouse monoclonal anti-cMyc (Upstate Biotechnology, Charlottesville, VA) antibodies. Immunocomplexes were subsequently incubated overnight with 60 $\mu$l of protein G agarose beads, and they were washed four times with ice-cold wash buffer (20 mM HEPES, 100 mM NaCl, 1 mM EDTA, 1% Nonidet P-40, and protease inhibitors). The proteins were eluted in 70 $\mu$l of Laemmli buffer by boiling for 5 min before immunoblotting. Immunoprecipitation from rat brain was performed similarly with the exception that 1 mg of rat brain membranes was solubilized in CHAPS buffer (50 mM Tris-HCl, 125 mM NaCl, 0.1 mM EGTA, 20 mM CHAPS, 2 mM dithiothreitol, and protease inhibitors) before immunoprecipitation with goat anti-D1 (Chemicon International, Temecula, CA) and immunoblotting with mouse anti-caveolin-1. Immunoprecipitated proteins were resolved by 12% SDS-PAGE under reducing conditions. Proteins were transferred to polyvinylidene difluoride before blocking in 5% skim milk for 1 h. Blots were incubated with the appropriate primary antibodies overnight (O/N) in 1% skim milk before incubation with HRP-conjugated secondary antibodies (Bio-Rad Laboratories, Hercules, CA) for 1.5 h. Immunoreactivity was detected by enhanced chemiluminescence using an ECL Plus kit (GE Healthcare, Chalfont St. Giles, Buckinghamshire, UK).

**Cell Surface Biotinylation.** Biochemical analysis of receptor endocytosis using cleavable biotin was performed as described previously (Cao et al., 1998) with some modifications. In brief, transfected cells were incubated with 0.5 mg/ml sulfo-NHS-SS-biotin (Pierce Chemical, Rockford, IL) for 40 min at RT. Cells were then rinsed 3 × 5 min with Tris-buffered saline to quench the biotinylation reaction. Biotinylated cells were then treated with 10 $\mu$M SKF 81297 for 30 min at 37°C to induce endocytosis. The remaining cell surface biotin was cleaved by washing cells with glutathione cleavage buffer (50 mM glutathione, 75 mM NaCl, 75 mM NaOH, and 10% fetal bovine serum) for 2 × 15 min at 4°C. Unreacted glutathione was subsequently quenched with 50 mM iodoacetamide (in PBS) for 3 × 5 min at 4°C. Cells were extracted in buffer containing 0.5% Triton X-100 (v/v), 10 mM Tris-Cl, pH 7.5, 120 mM NaCl, 25 mM KCl, and a protease inhibitor cocktail (Sigma-Aldrich) by rocking at 4°C for 3 h. The extracts were cleared of insoluble debris by centrifuging at 15,000*g* for 20 min. Receptors were immunoprecipitated from the clarified supernatant by incubating the lysate with 5 $\mu$g of anti-HA polyclonal antibody (BD Biosciences) O/N and then with 50 $\mu$l of protein G agarose PLUS beads (Pierce Chemical) for 3 h. Immunoprecipitations were washed sequentially with high salt buffer (0.1% SDS, 0.5% Triton X-100, 20 mM Tris-HCl, pH 7.5, 120 mM NaCl, and 25 mM KCl), 1 M NaCl in high salt buffer, and low salt wash buffer (10 mM Tris-HCl, pH 7.5) for 20 s/wash. Immunoprecipitated proteins were eluted by incubating in Laemmli buffer for 25 min at 37°C, and they were resolved by 12% SDS-PAGE under nonreducing conditions. Proteins were transferred to polyvinylidene difluoride before blocking in 5% skim milk O/N. Biotinylated receptors were detected by incubating membranes with Vectastain Elite ABC reagent (Vector Laboratories, Burlingame, CA) for 30 min followed by HRP detection with enhanced chemiluminescence.

**Membrane Preparation.** Transfected cells were washed extensively in PBS and centrifuged at 1500*g* to obtain a pellet. Cell lysates were prepared by polytron disruption in ice-cold 5:2 buffer, containing protease inhibitors. Lysates were centrifuged at 1000*g* for 10 min to separate nuclei and unbroken cells. Crude membrane fractions were prepared by centrifuging the supernatant at 20,000*g* for 25 min. Membrane protein was determined by the Bradford assay according to the manufacturer's instructions (Bio-Rad Laboratories).

**Radioligand Binding.** For whole cell binding experiments, transfected COS-7 cells were seeded onto 24-well plates (pretreated with poly-L-ornithine) at a density of $1.75 \times 10^5$ cells/well. Cells were preincubated with the appropriate treatments before exposure to agonist. Cells were washed with ice-cold buffer containing 1 mM EDTA and 50 mM Tris-HCl for 2 min to dissociate agonist before rinsing with 50 mM Tris-HCl for 1 min. Total binding was determined by incubating cells with 2 nM D1R antagonist [$^3$H]SCH23390 (prepared in antagonist binding buffer) on ice for 3 h. Nonspecific binding was defined by [$^3$H]SCH23390 binding in the presence of 1 $\mu$M (+)-butaclamol. Cells were subsequently washed with ice-cold wash buffer (50 mM Tris-HCl) for 3 × 1 min before lysing with 0.2 N NaOH for 20 min. Lysates were resuspended in scintillation fluid, and radioactivity was detected by an LS 6500 scintillation counter (Beckman Coulter, Fullerton, CA). For saturation binding analysis, membrane preparations (as described above) were used for radioligand binding at [$^3$H]SCH23390 concentrations of 4 nM, 1 nM, 500 pM, 100 pM, and 10 pM. Binding was performed at RT for 1.5 h before bound ligand was isolated by rapid filtration through a 48-well cell harvester (Brandel Inc., Gaithersburg, MD), using GF/C filters (Whatman, Maidstone, UK).

**Immunocytochemistry and Confocal Microscopy.** HEK293t cells cotransfected with D1R-GFP and cMyc-caveolin-1 were grown on glass coverslips in six-well plates until 20 to 40% confluence. Forty-eight hours after transfection, they were washed three times with PBS/0.2% bovine serum albumin (buffer B) and fixed with freshly prepared 4% paraformaldehyde. Cells were washed with 0.02 M glycine to quench remaining reactive aldehyde groups. The permeablization of cells was carried out in the presence of 0.1% saponin in PBS for 5 min. After blocking in buffer B for 1 h, fixed cells were washed with PBS, and then they were incubated with an anti-cMyc monoclonal antibody (1:1000; Upstate Biotechnology) for 2 h at RT. Cells were then washed two times in buffer B and once in PBS before incubating with tetramethylrhodamine B isothiocyanate-conjugated anti-mouse secondary antibody (Sigma-Aldrich) at 1:1000 dilution for 2 h at RT. Cells were then washed two times in buffer B and once in PBS for 5 min before glass coverslips were mounted. Images were acquired with a 63× lens on a Zeiss LSM510 confocal microscope (Carl Zeiss, Thornwood, NY). For the live cell monitoring of D1R and caveolin-1, HEK293t cells were cotransfected with cDNA encoding D1R-mRFP and caveolin-GFP for 48 h. To activate D1R, 10 $\mu$M SKF 81297 was administered to these cells, and confocal images were acquired every 2 to 5 min over an 80-min period using a 63× deep lens equipped on a Zeiss LSM510 confocal microscope.

**Bioluminescence Resonance Energy Transfer.** To detect interactions between D1R and caveolin-1, bioluminescence resonance energy transfer (BRET) studies were performed in which the D1R-Rluc fusion construct was cotransfected with increasing molar concentrations of caveolin-1-eGFP or empty vector eGFP (up to a 10-fold difference) in HEK293t cells. Cells were transfected in six-well plates and 24 h later, they were seeded into 96-well plates at a density of $5 \times 10^4$ cells/well. The following day, the substrate coelenterazine H (5 $\mu$M; Sigma-Aldrich) was added to each well to allow catalytic degradation by Rluc and subsequent light emission. Luminescence and fluorescence were measured separately at 480 and 535 nm, which corresponds to the Rluc and GFP maxima of the emission spectra, respectively, on a Victor3 microplate reader (PerkinElmer Life and Analytical Sciences) equipped with filters of the appropriate bandpass (Chroma Technology Corp., Rockingham, VT). The BRET ratio was defined as [(emission at 510–590 nm)/(emission at 440–500)] − Cf, where Cf corresponds to (emission at 510–590)/(emission at 440–500) for the *Rluc* construct expressed alone in the same experiment.

**cAMP Accumulation.** Basal and agonist-induced levels of cAMP were measured from $2.0 \times 10^5$ D1R-transfected COS-7 cells plated into 24-well plates. Cells were lysed in 0.1 N HCl for 20 min, and the supernatant was assayed for cAMP accumulation using an enzyme-linked immunoassay kit (Cayman Chemical, Ann Arbor, MI) according to the manufacturer's instructions. Where indicated, cells were pretreated with 2% methyl-β-cyclodextrin (mβCD) for 30 min followed by the addition of mβCD-cholesterol complexes (10 μg/ml cholesterol-mβCD complexes in a 1:6 M ratio) for 2 h to deliver cholesterol back into the cells. For desensitization experiments, cells expressing the indicated receptors were pretreated with 10 μM SKF 81297 for 20 min before stimulating with various concentrations of SKF 81297.

**GTPγS Binding Assays.** To quantify GTPγS binding to $G_s\alpha$, membrane preparations (100 μg/40 μl) of D1R-transfected COS-7 cells were incubated with a reaction mixture containing 2 nM [$^{35}$S]GTPγS and 10 μM GDP in the absence (basal) or presence of 10 μM SKF 81297. The reaction was incubated at 30°C for 1 min, and it was terminated with 1 ml of ice-cold assay buffer (10 mM HEPES, pH 7.4, 100 mM NaCl, 10 mM $MgCl_2$, and protease inhibitors). The samples were centrifuged at 20,000*g* for 6 min at 4°C. The resulting pellets were solubilized in 100 μl of ice-cold solubilization buffer (100 mM Tris, pH 7.4, 200 mM NaCl, 1 mM EDTA, 1.25% Igepal CA630, and protease inhibitors) and 0.18% SDS for 1 h at 4°C. Unsolubilized cellular debris was pelleted at 20,000*g* for 20 min. The supernatant was subsequently incubated with 5 μg of $G_s\alpha$ antibody O/N at 4°C, followed by addition of 70 μl of protein G agarose (Sigma-Aldrich) and mixing on a rotator for 4 h. Agarose beads were spun down at 2500 rpm for 3 min and washed four times with solubilization buffer. Beads were suspended in scintillation fluid, and radioactivity was determined.

**Data Analysis.** All pharmacological data were analyzed using Prism (GraphPad Software Inc., San Diego, CA). Saturation binding curves were generated using nonlinear least-squares regression curve fitting. Statistical analysis between group means was performed using one-way analysis of variance followed by Tukey's post hoc test.

## Results

**Cofractionation of D1R with Caveolin-1.** To determine whether D1R localizes in caveolae-related lipid raft domains, caveolin-enriched fractions were purified from COS-7 cell lysates expressing HA-tagged D1R using sucrose density gradient centrifugation. This fractionation scheme uses sodium carbonate to separate caveolin-enriched microdomains based on the high cholesterol and sphingolipid content that renders these fractions carbonate-insoluble with a low buoyant density. We validated the quality of our gradients by showing that all of the endogenously expressed caveolin-1 in COS-7 cells was recovered in fractions 4 and 5 (Fig. 1), which corresponded to the "light" vesicle or caveolae-enriched fractions (Igarashi and Michel, 2000), whereas clathrin heavy chain was localized exclusively in the high-density noncaveolae fractions (fractions 9–12). When the same fractions were analyzed for the subcellular distribution of D1R, a substantial fraction of D1 receptors (52 kDa) was found in the caveolin-enriched fractions, with some D1R recovery in noncaveolin-enriched fractions. A similar distribution of endogenous D1R was obtained when whole rat brain lysates were subjected to sucrose density gradient centrifugation (data not shown). This suggests that under basal conditions, a significant proportion of D1Rs were localized at the plasma membrane in caveolar microdomains. We also found that in COS-7 cells, the plasma membrane resident protein $Na^+/K^+$ ATPase cofractionated with caveolin-1, which is consistent with its functional dependence on the structural integrity of caveolae (Wang et al., 2004). It has also previously been shown to bind to caveolin-1, indicating that fraction 5 likely represents plasma membrane caveolin-enriched domains. ARF6, a GTP binding protein involved in vesicular trafficking, was found exclusively in the higher density fractions, suggesting that this protein is not involved in caveolar trafficking. $G_s\alpha$ was localized to both the caveolin-enriched fractions (fractions 4 and 5) as well as the high-density sucrose fractions, as expected (Li et al., 1995). Although $G_s\alpha$ and D1R did not colocalize precisely in the same fractions, the general observation that they were both localized in caveolin-enriched fractions suggests that functional G protein-coupled D1 receptors may be regulated in caveolae.

**D1R Interacted with Caveolin-1 in Heterologously Expressed Cell Lines and Rat Brain.** To assess whether localization of D1R in caveolin-enriched microdomains was due to a physical association between caveolin-1 and D1R, we used a two-pronged approach using coimmunoprecipitation and BRET assays. Coimmunoprecipation experiments were done in COS-7 cell lysates transiently coexpressing HA-tagged D1R and cMyc-tagged caveolin-1. Antibodies directed against HA coimmunoprecipitated cMyc-caveolin-1 (Fig. 2A, lane 3). Western analysis of recombinant caveolin-1 expression yielded a doublet of 24 and 21 kDa, which corresponds to the α and β isoforms of caveolin-1, respectively (Fig. 2A, lane 1). The specificity of these interactions was tested by immunoprecipitating with another IgG under identical conditions (Fig. 2A, mock); this did not yield a coimmunoprecipitate. It is unclear why COS-7 cells endogenously express only the α

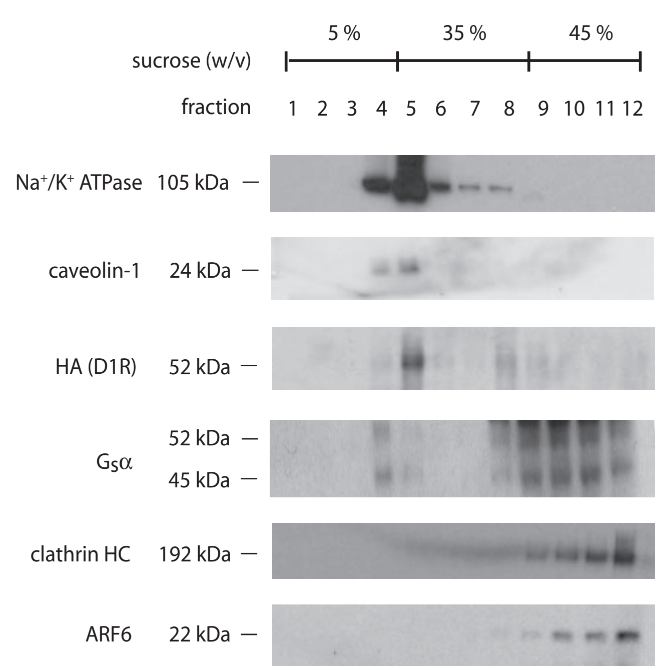


**Fig. 1.** Localization of D1R in caveolin-1-enriched fractions. Detergent-free sucrose density gradient fractions were prepared from D1R-transfected COS-7 cells, separated on SDS-PAGE, and probed with antibodies against the indicated proteins. D1R was found (as indicated by HA immunoreactivity) in both noncaveolin-1-enriched fractions and caveolin-1-enriched fractions (as indicated by the presence of caveolin-1 in fraction 5). Similar results were obtained when sucrose density gradient fractions from whole rat brain lysates were probed for endogenous D1R. Both $G_s\alpha$ and $Na^+/K^+$-ATPase were also found in caveolin-1-enriched fractions, whereas clathrin heavy chain and ARF6 was found exclusively in the high-density caveolin-1-free fractions.

isoform of caveolin-1 (Fig. 1), although this has been observed in other studies (Schwencke et al., 1999). Because the D1 receptor and caveolin-1 are prevalent in brain, we wanted to confirm the physiological nature of this interaction in whole rat brain tissue lysates. Immunoprecipitation with anti-D1R could only coprecipitate the $\alpha$ isoform of caveolin-1 (Fig. 2B, lane 2) despite the presence of both isoforms in brain (Fig. 2B, lane 1). When GFP-tagged D1R was coexpressed with cMyc-tagged caveolin-1 in HEK293t cells, both proteins were found to colocalize in various regions of the plasma membrane (Fig. 2C, merged) under basal conditions.

To evaluate the relative proximity of caveolin-1 and D1R, we used a BRET assay to show an interaction between these two proteins. BRET is based on the theory that bioluminescent energy transfer from the catalytic degradation of the substrate coelenterazine by a luciferase donor to a fluorescent acceptor requires an intermolecular distance of less than 50 Å; this distance posits a direct interaction between the

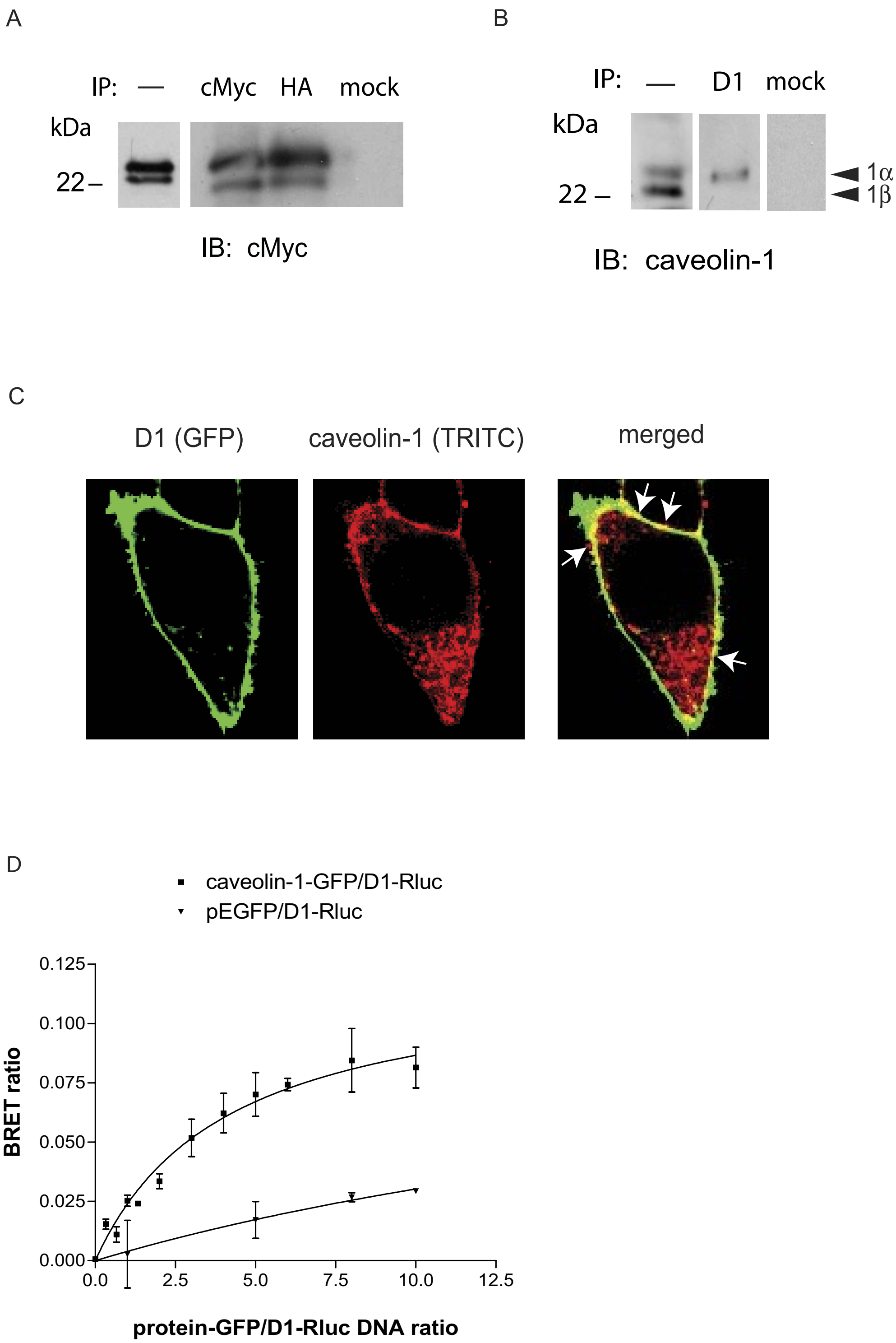


**Fig. 2.** D1R interacts with caveolin-1 in COS-7 cells and whole rat brain lysate. A, coimmunoprecipitation of D1R and caveolin-1 from lysates of COS-7 cells transfected with HA-tagged D1R and cMyc-tagged caveolin-1. Immunoprecipitations were performed with either monoclonal anti-cMyc, polyclonal anti-HA, or irrelevant IgG (mock), and then they were immunoblotted with a cMyc-specific monoclonal antibody. Immunoblot analysis in the absence of immunoprecipitating antibody is also shown (lane 1). B, coimmunoprecipitation of D1R and caveolin-1$\alpha$ from whole rat brain lysate. Immunoprecipitation was performed with monoclonal anti-D1R or irrelevant IgG (mock), and samples were subjected to immunoblots using monoclonal anti-caveolin-1. Both caveolin-1$\alpha$ and -1$\beta$ are expressed in whole rat brain homogenate (lane 1). C, HEK293t cells were cotransfected with D1R-GFP and cMyc-tagged caveolin-1, which was detected using a tetramethylrhodamine B isothiocyanate-conjugated secondary antibody. Cell surface colocalization of D1R-GFP and caveolin-1 is shown in the merged image (arrows). D, BRET saturation curves were generated from HEK293t cells cotransfected with a constant cDNA concentration of D1-Rluc and increasing concentrations of caveolin-1-GFP (■) or soluble GFP encoded by pEGFP vector (▼). The BRET, total fluorescence, and total luminescence were determined 48 h after transfection. The BRET levels were normalized against luminescent emission levels at 480 nm in the absence of GFP (background). Nonlinear regression analysis was performed to obtain a $B_{max}$ of 0.122 in cells cotransfecting D1R-Rluc and caveolin-1-GFP. The results are expressed as the mean BRET ratio ± S.E.M. of four to nine independent experiments carried out in replicates of six.

proteins being investigated. Energy transfer is typically quantified by an increase in the ratio of acceptor emission (GFP) to luciferase emission (Rluc). In this study, we used HEK293t cells (which are largely devoid of caveolin expression; Yamamoto et al., 1998) to avoid potentially confounding results from endogenous caveolin-1 interactions with D1R. The basal BRET was determined from HEK293t cells coexpressing constant levels of D1R-Rluc and increasing levels of caveolin-1-GFP (cav1-GFP) fusion protein (Fig. 2D). The BRET ratio increased as a hyperbolic function of the concentration of GFP fusion construct added, and it reached an asymptote that corresponded to a $BRET_{max}$ value of 0.122. The $BRET_{max}$ indicates the acceptor concentration required to attain maximum D1R/caveolin-1 coupling. This saturable characteristic indicates that the interaction between D1R and caveolin-1 was specific and not a result of random collisions that would otherwise yield a linear "bystander" BRET curve. In contrast, coexpression of D1R-Rluc with soluble GFP resulted in a negligible BRET signal that increased linearly with increasing expression levels of pEGFP vector.

**D1R Translocated to Caveolin-Enriched Fractions after Agonist Stimulation.** To test whether stimulation of the D1 receptor with agonist altered its localization in caveolin-enriched fractions, HA-D1R-transfected COS-7 cells were treated with the D1R agonist SKF 81297 for various time points, and the distribution of D1R was analyzed from subcellular fractions, as described above. As shown in Fig. 3, D1R localized to caveolin-enriched (fractions 4 and 5) and noncaveolin-enriched (fraction 8) fractions under basal conditions. Treatment of the D1 receptor with 10 $\mu$M SKF 81297 for 5 min increased the proportion of D1 receptors in caveolin-enriched fractions, with a concomitant decrease in D1 receptor recovery from noncaveolin-enriched fractions. Within 20 min of SKF 81297 stimulation, the majority of receptor protein (~70%) was localized in the caveolin-associated fractions, with a minor proportion of receptor in the noncaveolin-associated fractions. Densitometric analysis of the subcellular distribution of D1 receptors showed that there was no change in the total amount of protein recovered after agonist stimulation, indicating that the D1 receptor translocated from the noncaveolin-enriched fractions to the caveolin-enriched fractions. Similar findings were obtained when dopamine was used to stimulate the receptor (data not shown). The localization of endogenously expressed caveolin-1 did not change in response to SKF 81297 treatment.

**D1R Internalized through a Caveolar Pathway.** Based on the observation that the D1 receptor translocates to caveolin-enriched fractions after SKF 81297 stimulation, we

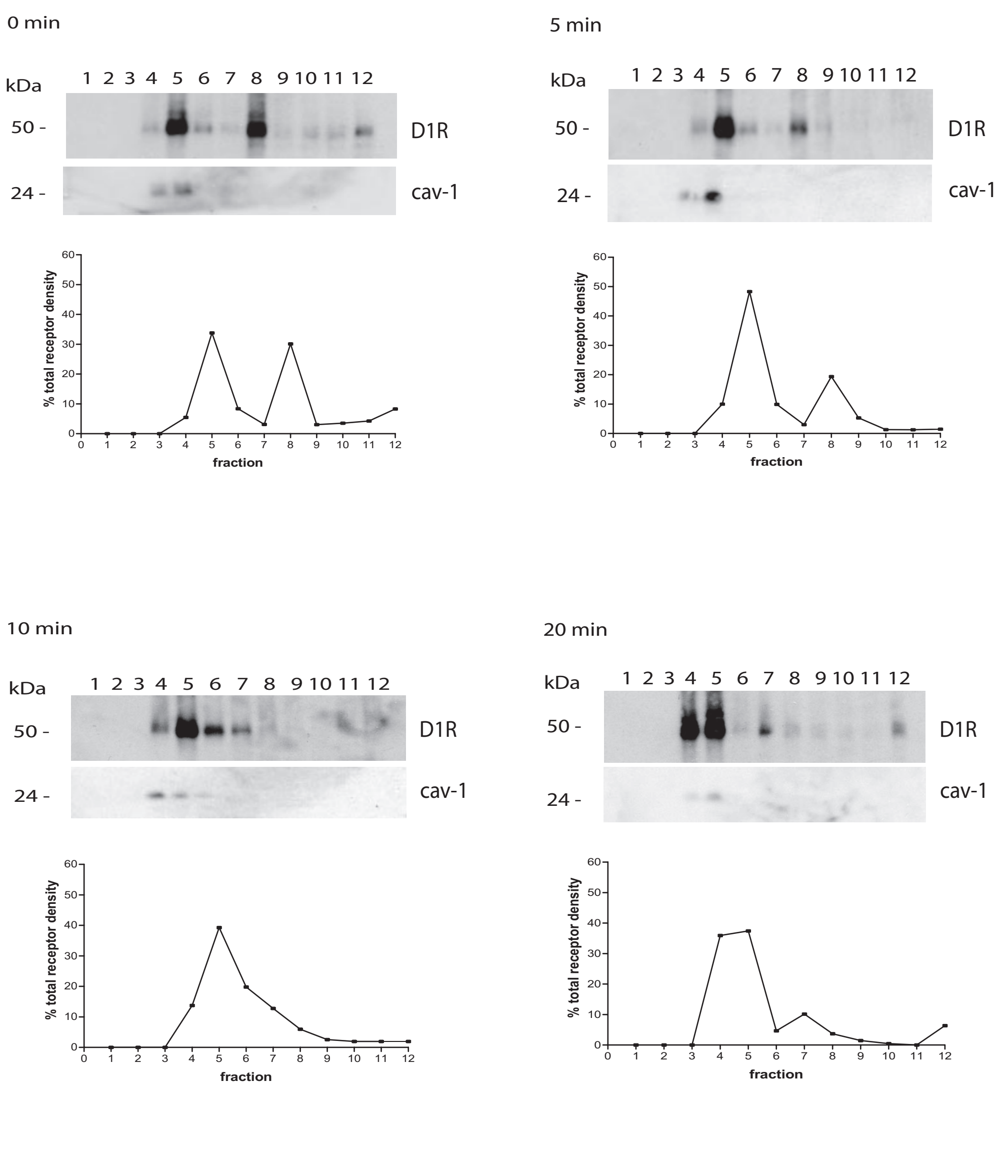


**Fig. 3.** Agonist-induced translocation of D1R into caveolin-1-enriched fractions. Detergent-free sucrose gradient subcellular fractions were prepared from HA-D1R-transfected COS-7 cells that were treated for various times (0, 5, 10, and 20 min) with the D1R agonist SKF 81297 at 10 $\mu$M. An equal volume of each fraction was separated on SDS-PAGE and analyzed by immunoblotting with antibodies directed against the HA epitope (top) or caveolin-1 (middle), as shown. No change in the distribution of caveolin-1 (fractions 4 and 5) was observed with agonist treatment. Semiquantitative analysis of D1R expression in each fraction was performed using densitometry (bottom).

wanted to determine whether this might be attributed to agonist-dependent D1R endocytosis. Although clathrin-dependent internalization has been shown to be the major endocytic pathway for many GPCRs, including the D1 receptor in HEK293t cells (Vickery and von Zastrow, 1999), endocytosis through caveolae has also been reported to be an alternative route for the cellular entry of certain GPCRs. Although both processes seem to be dynamin-dependent, it has been suggested that although clathrin-dependent endocytosis is dependent on phosphorylation by GRK and arrestin binding, caveolar endocytosis depends on phosphorylation by protein kinase A (PKA) (Rapacciuolo et al., 2003). To address this, we performed whole cell radioligand binding assays and cell surface biotinylation studies to quantify the degree of D1 receptor internalization in the presence of various inhibitors of caveolar and clathrin-mediated endocytic pathways. In whole cell binding assays, D1R-transfected COS-7 cells were preincubated with hypertonic sucrose or concanavalin A, both of which are known inhibitors of clathrin-mediated endocytosis, or m$\beta$CD, a cholesterol depleter known to disrupt caveolae structure and function. Whole cell surface binding of [$^3$H]SCH23390, a selective D1R antagonist, to D1 receptors was compared before and after 30-min incubation with 10 $\mu$M SKF 81297 in the presence of these compounds. Pretreatment of cells with sucrose or concanavalin A did not significantly alter the degree of D1 receptor internalization (Fig. 4A). Likewise, transfection of the D1 receptor with a dominant-negative mutant of GRK2, K220R, did not change the extent of internalization even when overexpressed. This suggests that clathrin-mediated internalization is not the only endocytic route used by the D1 receptor. In contrast to this, pretreatment with 2% m$\beta$CD almost abolished agonist-induced internalization. The concentration and treatment time of m$\beta$CD used does not affect COS-7 cell viability (McCabe and Berthiaume, 2001). Consistent with this, cotransfection of the D1 receptor with a dominant-negative mutant of caveolin-1, P132L (cav1-P132L), significantly attenuated D1R internalization by approximately 38%. To determine whether D1R internalization was PKA-dependent, we tested the effects of H89, a PKA-selective inhibitor, on receptor sequestration. The inhibition of PKA function yielded a minor, but insignificant, decrease in agonist-mediated internalization.

To further evaluate whether D1R internalized through a caveolar pathway, we used glutathione-cleavable biotin to assess the amount of internalized receptor after caveolae disruption and agonist stimulation (Fig. 4B). The radioligand binding experiments described above were used to show changes in cell surface binding in response to caveolae disruption and agonist stimulation. Hence, we conducted cell surface biotinylation assays to show that these changes were actually due to differences in the amount of receptor internalized. In brief, D1R-transfected cells were pretreated with cell-impermeable cleavable biotin before stimulation with agonist. All cell surface-bound biotin was then stripped with glutathione, leaving only internalized biotinylated receptors protected from glutathione cleavage. These internalized receptors were then detected by immunoprecipitation and Western blot analysis. As shown in Fig. 4B, D1R stimulation with 10 $\mu$M SKF 81297 triggered an increase in internalized receptor (lane 3). In contrast, pretreatment of cells with m$\beta$CD or filipin, a sterol-binding agent that inhibits caveolae formation, attenuated the amount of internalized biotinylated receptor detected. Similar results were obtained when cells were cotransfected with cav1-P132L, indicating that this attenuation was specifically a result of caveolae disruption. Because caveolar translocation occurs within 20 min of agonist induction (Fig. 3), it seems likely that D1R translocates to caveolae upon binding to agonist before undergoing caveolar endocytosis.

**Kinetics of Caveolar Internalization of D1R.** Because D1R internalization in COS-7 cells was insensitive to inhib-

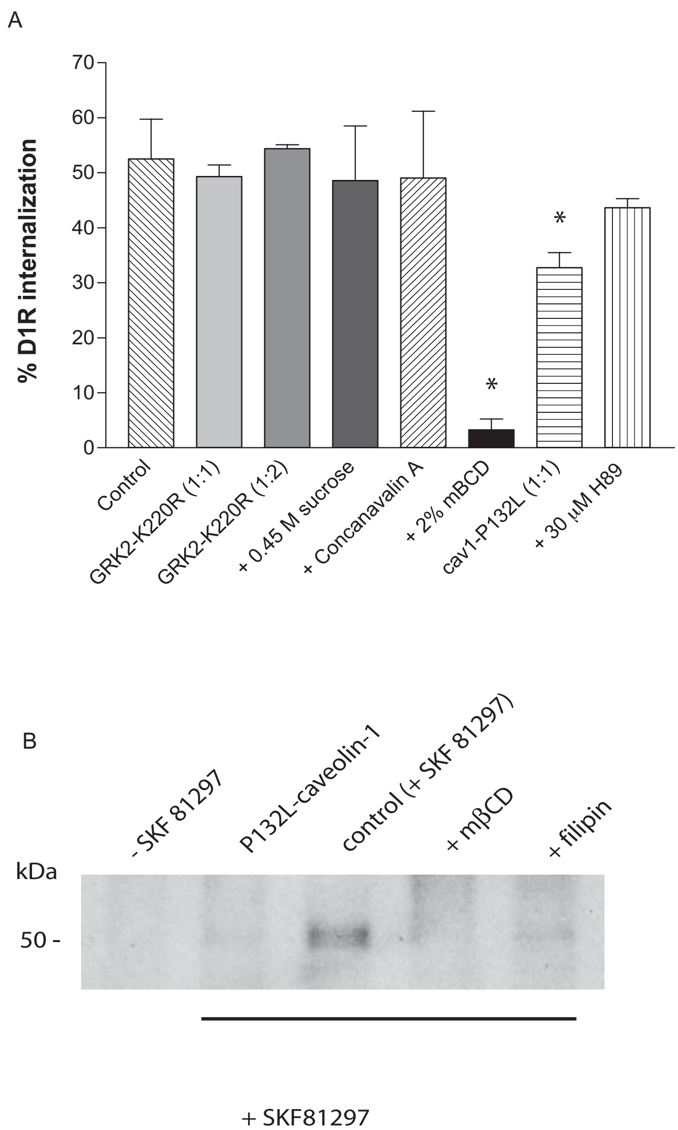


**Fig. 4.** Agonist-induced internalization of D1R into caveolae. A, HA-D1R-expressing cells were either coexpressed with GRK2-K220R at a 1:1 and 1:2 transfection ratio or caveolin-1 P132L (cav1-P132L), or they were pretreated with 0.45 M sucrose, 0.25 mg/ml concanavalin A, 2% m$\beta$CD, or 30 $\mu$M H89 for 30 min before agonist stimulation with 10 $\mu$M SKF 81297 for an additional 30 min. Receptor density was estimated by whole cell radioligand binding analysis with 2 nM [$^3$H]SCH23390. The results are expressed as the mean percentage of internalization ± S.E.M. of three to five independent experiments. Significance at $p < 0.05$ versus percentage of internalization under control conditions is denoted by asterisk (*). B, HA-D1R-expressing cells were either coexpressed with caveolin-1 P132L, or they were pretreated with 2% m$\beta$CD or 1 $\mu$g/ml filipin before cell surface biotinylation was performed. Cells were stripped of biotin after stimulation with agonist for 30 min (and in the absence of agonist, lane 1), and internalized receptors were immunoprecipitated with polyclonal anti-HA before analysis on SDS-PAGE.

itors of clathrin-mediated endocytosis but attenuated by known disrupters of caveolar function, we concluded that the D1 receptor probably undergoes caveolar endocytosis in this cell line. To quantify the internalization kinetics of the D1 receptor through caveolae, we measured the extent of receptor internalization over a fixed period using binding assays. After 5 min of receptor stimulation with 10 $\mu$M SKF 81297, approximately 20% of the cell surface population of D1 receptors was internalized (Fig. 5A). Maximum internalization was achieved at 45 min where approximately 55% of receptors were internalized. This indicates that caveolar endocytosis of D1R is a kinetically slower process than clathrin-mediated endocytosis of D1R, the latter of which occurs more rapidly with approximately 65% receptor internalization occurring within 5 min of agonist stimulation (Vickery and von Zastrow, 1999).

To monitor the intracellular distribution of the D1 receptor in caveolae, we used real-time live cell imaging D1R-mRFP and caveolin-1-GFP. In the absence of agonist, D1R-mRFP exhibited a predominantly cell surface distribution, whereas caveolin-1-GFP was localized to both cell surface and perinuclear regions (Fig. 5B, top row). Within 20 min of incubation with agonist at 37°C, the appearance of distinct vesicles containing caveolin-1-GFP and D1R-mRFP originating from the cell surface could be observed (Fig. 5B, second row). These vesicles, presumably caveolae, were found to redistribute to intracellular regions upon continuous agonist exposure with the colocalization of caveolin-1 and D1R maintained throughout the endocytic process. These vesicles could be seen trafficking back to the cell surface within 40 min, ultimately returning to the plasma membrane within 60 min of initial agonist stimulation. This may implicate an additional role for caveolae in D1R recycling.

**D1R Cell Surface Expression Was Dependent on the Distal Aromatic Residue of the Putative Caveolin Binding Motif.** Because caveolae-associated proteins require an intact caveolin binding motif to interact with caveolin-1 (Couet et al., 1997), we designed several D1R mutants by site-directed mutagenesis in which the critical amino acids within the putative caveolin binding motif (CBM) in the proximal half of the seventh TM domain were disrupted. This motif lies just upstream of the highly conserved NPXXY motif. The F313A, W318A, and W321A mutants disrupted the CBM at the proximal, central, and distal aromatic residues, respectively, whereas the FWW/A mutation had all three aromatic residues substituted for alanine. Plasma membrane expression of HA-tagged CBM mutants was assessed through cell surface biotinylation (Fig. 6). The F313A and W318A mutants were found to have slightly higher and lower plasma membrane expression than wild-type D1R, respectively. In contrast, cell surface expression of the W321A and FWW/A mutants was strongly attenuated compared with wild-type D1R, possibly due to protein misfolding. To assess whether the pharmacological properties of the CBM mutants were altered, saturation binding analysis was performed on F313A and W318A. These single point mutants displayed high-affinity binding for [$^3$H]SCH23390, with $K_d$ values of 0.57 and 0.61 nM, respectively, which is comparable with that of wild-type D1R (Table 1). The $B_{max}$ values were 1.8 and 0.86 pmol/mg membrane protein, respectively, with relative receptor densities that correlated with plasma membrane receptor expression as determined by cell surface biotinylation. The triple substitution mutant FWW/A exhibited negligible binding, which was consistent with the marked decrease in cell surface expression. This failure to translocate to the plasma membrane was probably attributed to the distal aromatic residue Trp321, because this mutant similarly exhibited a poor binding and expression profile.

**D1 Dopamine Receptor Mutants Lacking an Intact Caveolin Binding Motif Failed to Internalize.** To further define the role of the caveolin binding motif in the D1R, we performed internalization studies using whole cell binding assays on the various CBM mutants (Fig. 7A). Preincubation of cells expressing the wild-type D1 receptor with 10 $\mu$M SKF 81297 for 30 min resulted in a loss of 57.7 ± 3.3% of cell surface receptors. In contrast, the extent of receptor internalization for F313A and W318A was significantly reduced to 15.4 ± 4 and 4.5 ± 6.7%, respectively. We could not accurately determine the extent of internalization for W321A because of its poor expression. To determine whether F313A and W318A could interact with caveolin-1, we performed BRET competition experiments in which untagged F313A and W318A were individually tested for their ability to reduce the BRET signal generated between D1R-Rluc and cav1-GFP. The selected CBM mutants were cotransfected with an amount of D1R-Rluc and cav1-GFP found to generate a near maximal BRET signal (Fig. 2D). We transfected a specific amount of cDNA that was optimized for each mutant receptor and that was not found to compromise cav1-GFP or D1R-Rluc expression. Expression of untagged wild-type D1R markedly reduced the BRET signal generated by D1R-Rluc and cav1-GFP (Fig. 7B). In contrast, expression of either untagged F313A or W318A did not significantly affect the BRET signal between the two fusion proteins. Equivalent expression of transfected F313A and W318A was confirmed by radioligand binding assays (data not shown). These data suggest that the D1R interacts with caveolin-1 through a series of aromatic amino acids defined by a putative caveolin binding motif and that the integrity of this motif is critical in mediating caveolar endocytosis.

**Cholesterol Depletion Did Not Alter $G_s$-Mediated Production of cAMP through D1R.** Based on the observation that $G_s\alpha$ and adenylyl cyclase (Head et al., 2006) colocalized with the D1 receptor in caveolin-enriched sucrose gradient fractions (Fig. 1), we sought to investigate the role of caveolin-1 on D1R-mediated cAMP signaling. Using an enzyme-linked immunosorbent assay, we wanted to determine what effect caveolar disruption would have on the ability of the D1R to activate adenylyl cyclase and to enhance cAMP production. Cells expressing D1R were pretreated with 2% m$\beta$CD before stimulating with various concentrations of SKF 81297 for 20 min. There was no significant difference between the $EC_{50}$ of the dose-response curves for cAMP generation (Fig. 8A), and there were no significant differences between the $K_d$ for SCH23390 and $B_{max}$ of D1R in the presence or the absence of m$\beta$CD (Table 1). However, we found that there was an approximately 35% increase in cAMP at the highest concentration of SKF 81297 used (corresponding to the $V_{max}$) in the presence of m$\beta$CD (Fig. 8A). This enhancement was reversed upon cholesterol replenishment as described under *Materials and Methods* (data not shown). Likewise, cotransfection of cav1-P132L at a 4-fold cDNA concentration over that of D1R was also found to enhance the $V_{max}$ of cAMP accumulation by approximately 43% without

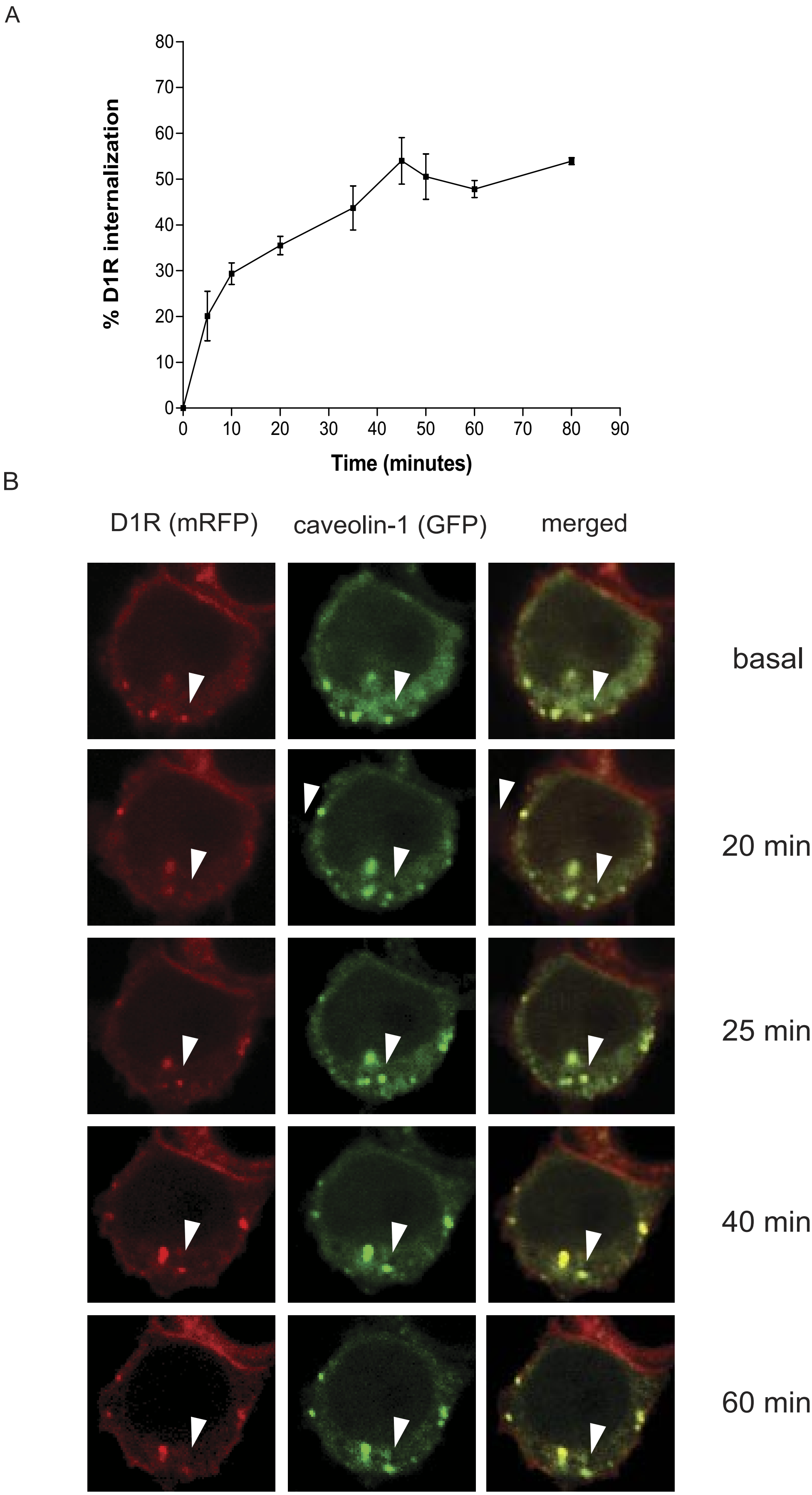


**Fig. 5.** Kinetics of D1R internalization via caveolae. A, whole cell radioligand binding analysis was performed with 2 nM [$^3$H]SCH23390 on D1R-expressing cells exposed to 10 $\mu$M SKF 81297 for the indicated times. Results are expressed as the mean percentage of internalization ± S.E.M. of three independent experiments. B, HEK293t cells were cotransfected with D1-mRFP and caveolin-1-GFP. Shown are live cell confocal microscopy images obtained over a 60-min period of 10 $\mu$M SKF8 1297 treatment in serum-free minimum essential medium. Colocalization of D1R-mRFP and caveolin-GFP is shown in the merged image (yellow) and maintained throughout the duration of agonist treatment (arrowhead).

significantly altering the $EC_{50}$ (Fig. 8B). To test the hypothesis that the enhancement in cAMP production was $G_s$-mediated and not due to a global dysregulation of adenylyl cyclase, [$^{35}$S]GTP$\gamma$S binding assays, which serve as a measure of receptor mediated G protein activation, were performed in D1R-transfected and untransfected cells in the presence and absence of 2% m$\beta$CD. Stimulation of D1R-transfected cells with 10 $\mu$M SKF 81297 for 1 min increased [$^{35}$S]GTP$\gamma$S binding to $G_s$ by 47 ± 5.9% compared with basal levels (Fig. 8C). In contrast, basal [$^{35}$S]GTP$\gamma$S binding to $G_s$ from m$\beta$CD-treated D1R-transfected cells was more than 2-fold higher (114 ± 52.4%) than in untreated cells. When membranes from these cholesterol-depleted cells were incubated with 10 $\mu$M SKF 81297, no further increase in [$^{35}$S]GTP$\gamma$S binding was observed (basal, 114 ± 52.4% over m$\beta$CD-untreated versus + SKF 81297, 113 ± 41.5% over m$\beta$CD-untreated). No changes in [$^{35}$S]GTP$\gamma$S binding were observed in untransfected cells in the presence of m$\beta$CD (data not shown). Together, these data suggest that caveolar disruption activates $G_s$ maximally without altering cAMP levels. This constitutive activation of $G_s$ occurred independently of agonist binding, which was required for cAMP production.

**Caveolin Binding Mutants Exhibited Constitutive Desensitization.** To further characterize the effect of disrupting the association of D1R with caveolae, we wanted to determine whether the interaction with the caveolin-1 protein itself was essential for cAMP signaling. Contrary to the effects of cholesterol depletion on cAMP production, both the F313A and W318A mutants displayed an equally small, but significant, increase in the $EC_{50}$ for cAMP generation compared with wild-type D1R (Fig. 9A). The $EC_{50}$ for cAMP generation was determined to be $4.8 \times 10^{-7}$, $1.8 \times 10^{-6}$ M, and $2.3 \times 10^{-6}$ M for wild-type D1R, F313A, and W318A, respectively. Furthermore, the F313A mutant displayed an approximately 25% decrease in $V_{max}$ compared with wild-type D1R when values were corrected against the cell surface receptor density. The W318A mutant did not show any difference in its capacity to maximally stimulate cAMP. We tested the hypothesis that these receptor mutants might be constitutively desensitized as a result of their diminished ability to efficiently produce cAMP. Stimulation of cells (pretreated with 10 $\mu$M

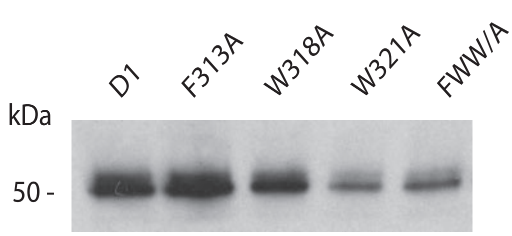


**Fig. 6.** Cell surface expression of D1R mutant receptors lacking an intact caveolin binding motif. Plasma membrane expression of HA-tagged D1R mutant receptors with a disrupted caveolin binding motif was assessed by cell surface biotinylation and immunoprecipitation with anti-HA-specific antibodies. The result is representative of three independent experiments.

TABLE 1

[$^3$H]SCH23390 binding parameters for wild-type D1R and mutant receptors lacking an intact caveolin binding motif

For each construct, results are reported as the mean ± S.E.M. of at least three independent experiments.

| | $B_{max}$ | $K_d$ |
|---|---|---|
| | *pmol/mg membrane protein* | *nM* |
| Wild type | 1.22 ± 0.1 | 0.26 ± 0.02 |
| F313A | 1.80 ± 0.1 | 0.57 ± 0.05 |
| W318A | 0.86 ± 0.1 | 0.61 ± 0.03 |
| W321A | N.A. | N.A. |
| FWW/A | N.A. | N.A. |
| +m$\beta$CD | 1.19 ± 0.1 | 0.37 ± 0.08 |

N.A., not available.

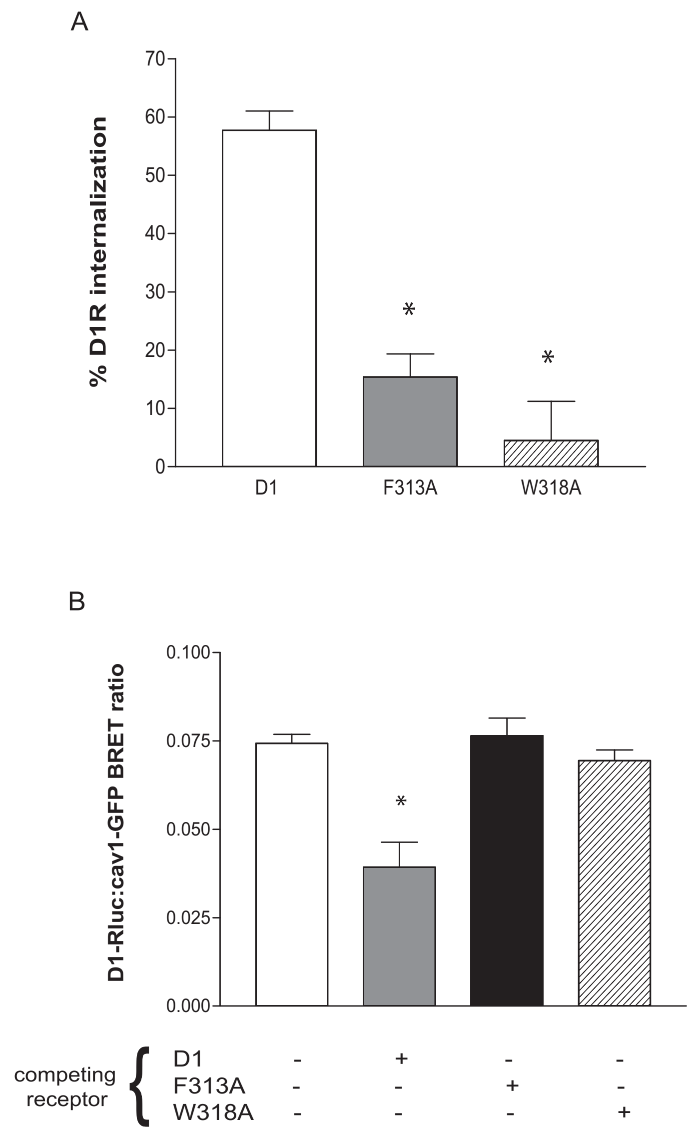


**Fig. 7.** Caveolar internalization of D1R requires an intact caveolin binding motif. A, COS-7 cells were transfected with wild-type D1R, F313A, or W318A, and then they were treated with 10 $\mu$M SKF 81297 for 30 min before receptor density was estimated by whole cell radioligand binding analysis with 2 nM [$^3$H]SCH23390. Results are expressed as the mean percentage of internalization ± S.E.M. of at least three independent experiments. Significance at $p < 0.05$ versus percentage of internalization of wild-type D1R is denoted by asterisk (*). B, BRET experiments were performed by cotransfecting D1R-Rluc and caveolin-1-GFP at a ratio (1:7) found to give a near-maximal energy transfer signal. Coexpression of the D1R-Rluc/caveolin-1-GFP pair with a 2-fold excess over D1R-Rluc of either untagged D1R, F313A, or W318A was performed to competitively disrupt BRET between D1R-Rluc and caveolin-1-GFP. The results are expressed as the mean BRET ratio ± S.E.M. of three to four independent experiments carried out in replicates of six. Significance at $p < 0.05$ versus BRET between D1-Rluc and caveolin-1-GFP.

SKF 81297 for 20 min) expressing wild-type D1R shifted the $EC_{50}$ to the right by over half a log unit while reducing the $V_{max}$ by 33% (Fig. 9B). However, stimulation of agonist-pretreated cells independently expressing either F313A or W318A did not result in any significant changes in the $EC_{50}$ (F313A, $1.29 \times 10^{-6}$ M; W318A, $1.65 \times 10^{-6}$ M). Furthermore, although the $V_{max}$ of agonist pretreated F313A was not altered, the $V_{max}$ of pretreated W318A was significantly attenuated by approximately 26%. This suggests that F313A was constitutively desensitized, whereas W318A exhibited only partial constitutive desensitization. Taken together, these results suggest that caveolin-1 binding to D1R is required to inhibit constitutive desensitization, possibly by regulating autophosphorylation.

## Discussion

In this study, we report that the D1 dopamine receptor interacts with caveolin-1 in brain and undergoes agonist-induced endocytosis through caveolae, which is dependent on the direct interaction of caveolin-1 with the D1 receptor. The stimulation of the D1 receptor with the full agonist SKF 81297 triggered a robust translocation of receptor to caveolin-enriched fractions and a concomitant decrease in expression in noncaveolin-enriched fractions without any change in the distribution of caveolin-1 after agonist treatment. We identified a caveolin binding motif in the proximal half of transmembrane domain 7 of the D1 receptor, which was shown to be critical for the interaction between the receptor

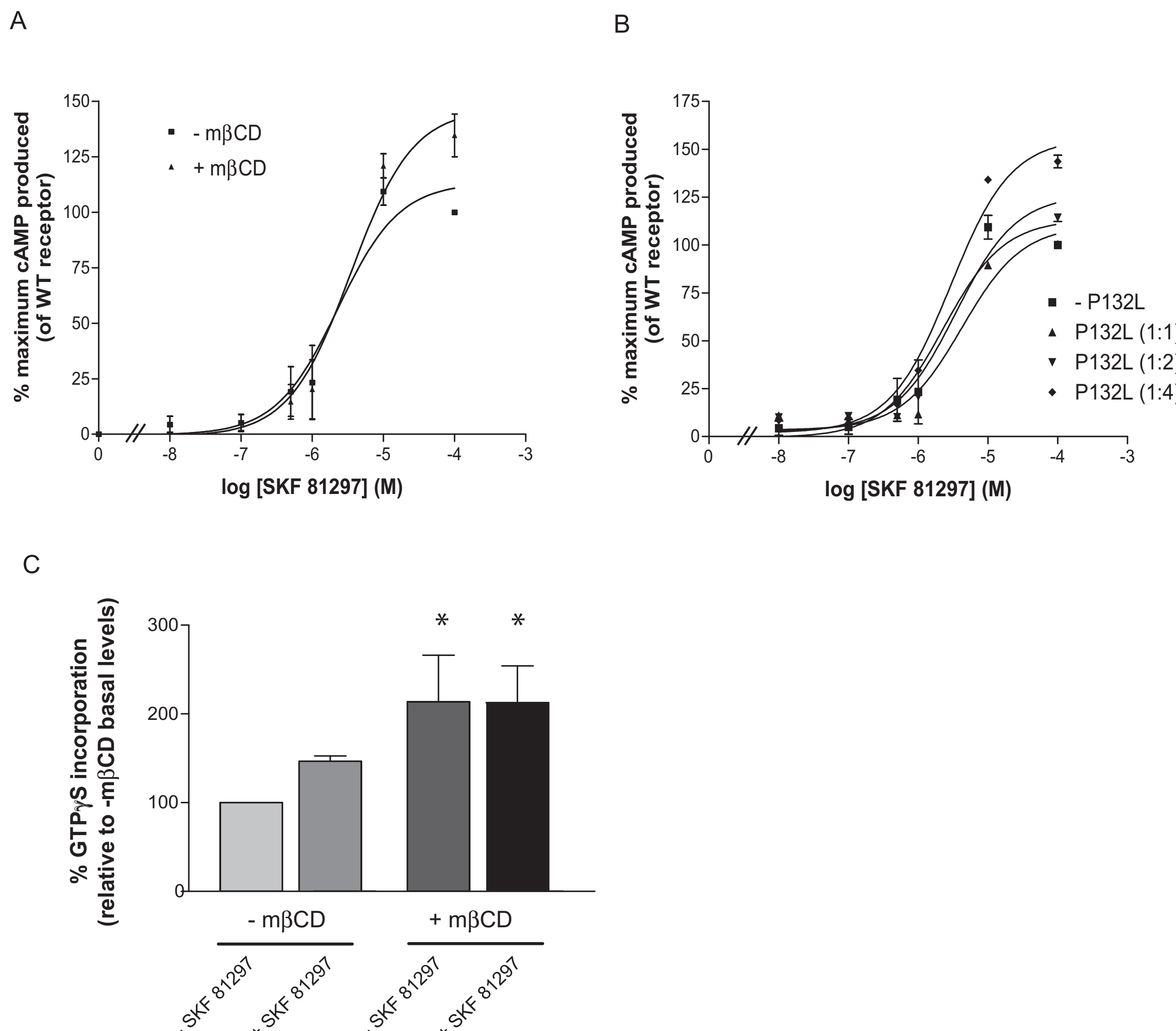


**Fig. 8.** Caveolar disruption enhances D1R-mediated cAMP production. A, D1R-transfected COS-7 cells were pretreated with vehicle (−mβCD) or with 2% mβCD for 30 min before cells were challenged with 0, 10 nM, 100 nM, 500 nM, 10 μM, or 100 μM SKF 81297 for 20 min. The results are expressed as the mean percentage of cAMP accumulation ± S.E.M. relative to maximum cAMP levels of wild-type D1R in the absence of mβCD. B, D1R was coexpressed with increasing cDNA concentrations of cav1-P132L at D1R:cav1-P132L transfection ratios of 1:1, 1:2, and 1:4 before cells were challenged with increasing concentrations of SKF 81297 ($10^{-8}$–$10^{-4}$). The results are expressed as the mean percentage of cAMP accumulation ± S.E.M. relative to maximum cAMP levels of wild-type D1R in the absence of cav1-P132L (−P132L). C, membranes from D1R-transfected cells were prepared and vehicle- or SKF 81297-stimulated [$^{35}$S]GTPγS binding to $G_s$ was determined. The results are expressed as the mean percentage of [$^{35}$S]GTPγS binding relative to basal binding levels in the absence of mβCD. Significance at $p < 0.05$ versus percentage of SKF 81297-induced [$^{35}$S]GTPγS binding in the absence of mβCD is denoted by asterisk (*).

and caveolin-1, and the mutation of which was found to abrogate agonist-induced receptor internalization. Furthermore, we demonstrate that the structural integrity of caveolae also seems to be important for regulating agonist mediated D1R production of cAMP.

We used coimmunoprecipitation and BRET saturation assays to show that D1R and caveolin-1 exist in a functional complex. We adapted the BRET assay for use in live cells to show that caveolin-1 and the D1 receptor interacted in a specific and saturable manner. In whole rat brain, we detected a selective coprecipitation of the $\alpha$ isoform of caveolin-1 by the D1 receptor, implicating a physiological preference for the $\alpha$ isoform over the $\beta$ isoform, which was not observed in COS-7 cells. The full-length $\alpha$ and truncated $\beta$ isoforms of caveolin-1 are derived from the same cDNA, although from different methionine start sites, and they differ by the first 31 N-terminal amino acid residues. It is unlikely that these residues are critical for the interaction of caveolin-1 with the D1 receptor, because both isoforms were coprecipitated in our heterologous cell expression assays. Instead, despite both isoforms being present in brain, it is possible that the $\alpha$ isoform is the only caveolin-1 isoform that is expressed in regions of the brain where the D1 receptor is expressed. On the other hand, D1 receptors may selectively

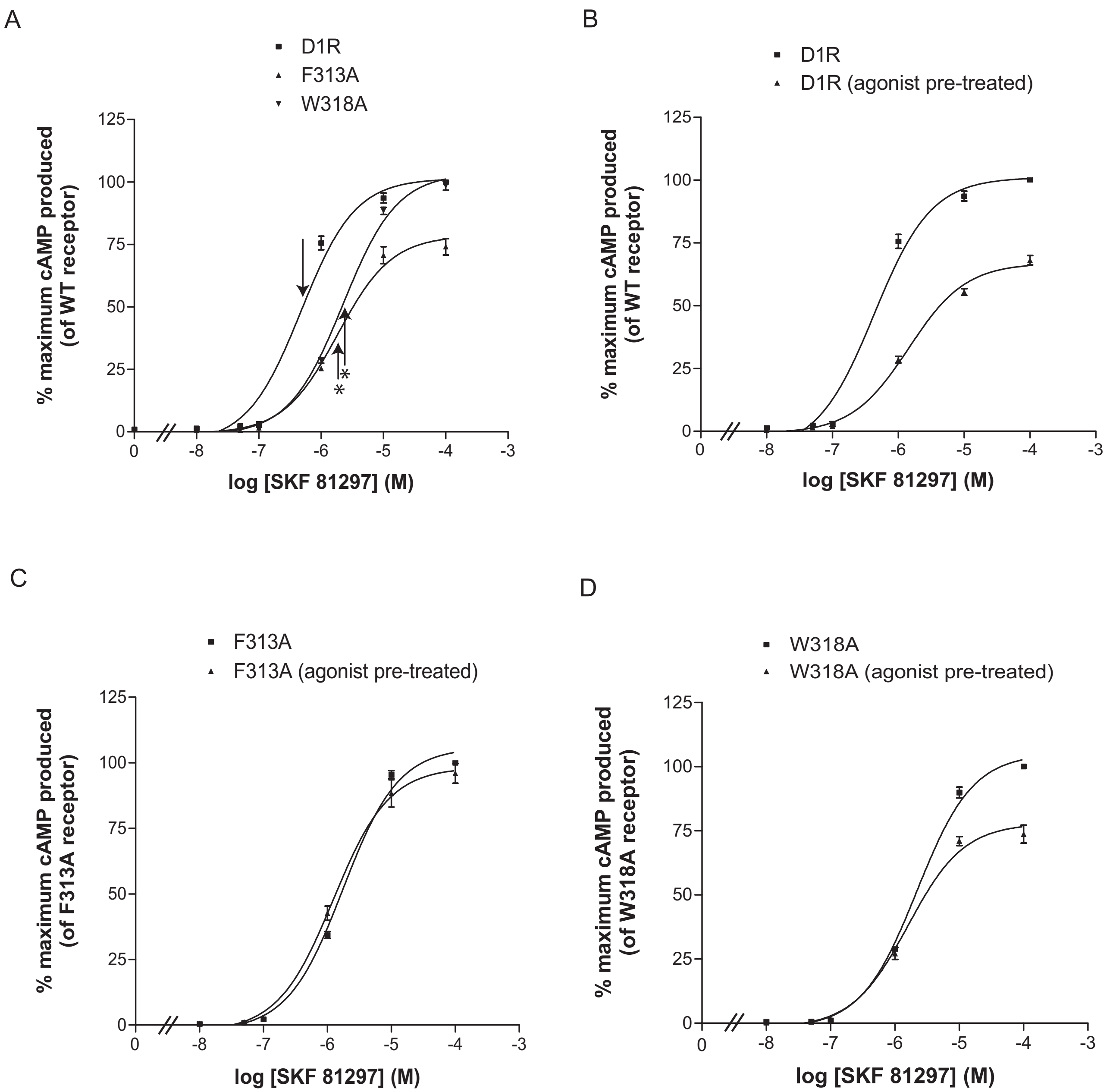


**Fig. 9.** Caveolin binding mutants are constitutively desensitized. A, D1R-, F313A-, or W318A-transfected COS-7 cells were challenged with 0, 10 nM, 100 nM, 500 nM, 10 $\mu$M, or 100 $\mu$M SKF 81297 for 20 min to stimulate cAMP production. The results are expressed as the mean percentage of cAMP accumulation ± S.E.M. relative to maximum cAMP levels of wild-type D1R. Arrows indicate $EC_{50}$. Significance at $p < 0.05$ versus $EC_{50}$ of D1R is denoted by asterisk (*). B, cells transfected with D1R were pretreated with 10 $\mu$M SKF 81297 for 20 min before being challenged with increasing concentrations of SKF 81297 ($10^{-8}$–$10^{-4}$). The desensitization profiles of F313A (C) and W318A (D) were also determined in a similar manner. The data are presented as the mean percentage of cAMP accumulation ± S.E.M. relative to maximum cAMP levels of the receptor indicated in the absence of agonist pretreatment.

cosegregate with caveolin-1$\alpha$ if caveolin-1$\alpha$-containing caveolae favor the sequestration of signaling components involved in D1 receptor function (Fujimoto et al., 2000; Nohe et al., 2005).

To further study the interaction with caveolin-1, we generated D1 receptor mutants in which the putative caveolin binding motif in TM 7 was disrupted. Although the pharmacological properties of the point mutants F313A and W318A were preserved, there was a significant reduction in the cell surface expression of the other mutants that did not permit pharmacological characterization. The FWW/A triple mutant was poorly expressed; we determined that in the D1 receptor, the distal aromatic amino acid of the caveolin binding motif, Trp321, is probably the critical residue maintaining proper receptor expression, because this mutation yielded a low expression profile compared with FWW/A. Similar mutations in the angiotensin II type 1 receptor also abrogated receptor plasma membrane expression, suggesting that caveolin-1 may act as a chaperone for exocytic transport of the $AT_1$ receptor to the cell surface (Wyse et al., 2003). This is unlikely to be the case for the D1 receptor, because both F313A and W318A expressed robustly, but they were unable to interact with caveolin-1 as demonstrated by their inability to competitively disrupt the BRET signal between D1-Rluc and cav1-GFP. However, consistent with the requirement for a physical association with caveolin, these receptors were not able to internalize as efficiently as wild-type D1 receptor, suggesting that caveolar internalization of D1 receptors may require an interaction with caveolin-1.

Besides the classic endocytic pathway involving clathrin-coated pits, other ligand-induced internalization pathways have been described that involve caveolae (Chini and Parenti, 2004) and other clathrin/caveolae-independent mechanisms (Roseberry and Hosey, 2001). To determine whether the agonist-induced targeting of the D1 receptor to caveolin-enriched sucrose fractions could be attributed to caveolar endocytosis, D1 receptor-expressing cells were challenged with various known inhibitors of caveolae function before stimulation with SKF 81297. Quantification of cell surface D1 receptors by radioligand binding analysis showed that agonist-induced receptor internalization was significantly inhibited by pretreatment with methyl-$\beta$-cyclodextrin. The cholesterol-depleting effects of this treatment were specific to caveolae, because coexpression with dominant-negative caveolin-1 P132L yielded a similar effect. These results were strengthened by reversible cell surface biotinylation studies in which filipin was also shown to suppress receptor internalization. The inhibition of clathrin-dependent endocytosis by hypertonic sucrose, concanavalin A, or the dominant-negative G protein-coupled receptor kinase 2 mutant K220R did not affect the extent of internalization, suggesting that in COS-7 cells, this may not be the dominant mode of D1 receptor internalization. Although these cells express low levels of arrestin and GRK2, the endogenous expression levels of these proteins in COS-7 cells are sufficient to facilitate arrestin- and clathrin-mediated internalization of various other GPCRs (Vrecl et al., 1998; Gáborik et al., 2001), indicating that both internalization pathways are functional in this cell line. Therefore, the D1 dopamine receptor is fully capable of internalizing through the clathrin-coated pit pathway (Vickery and von Zastrow, 1999), as well as through caveolae. However, the molecular determinants that control which endocytic route (clathrin versus caveolae) is taken remain unclear. A previous study reported that clathrin-mediated endocytosis was mediated by GRK phosphorylation, whereas caveolae-dependent endocytosis was controlled by PKA phosphorylation (Rapacciuolo et al., 2003); both GRK- (Lamey et al., 2002) and PKA (Mason et al., 2002)-induced phosphorylation have been shown to occur in the D1 receptor after agonist activation. Our data showed that the extent of D1 receptor internalization was not significantly affected by PKA inhibition, suggesting that other PKA-independent mechanisms, such as cholesterol oxidation, might dictate caveolae-mediated endocytosis (Okamoto et al., 2000).

In our studies, we showed that although caveolae disruption by cholesterol depletion or overexpression with cav1-P132L did not alter the receptor's affinity or the $EC_{50}$ for cAMP generation, the $V_{max}$ was significantly enhanced. This was not consistent with the dose-response profile exhibited by F313A and W318A, the former of which showed an attenuated $V_{max}$, and both of which showed a decrease in the $EC_{50}$ for agonist-mediated cAMP production. Although it is difficult to reconcile these differences, the effects of disrupting caveolae may not be equivalent to disrupting caveolin interactions when characterizing the $G_s$-cAMP signaling pathway. Indeed, our results suggest that these mutants' inability to interact with caveolin-1 renders a constitutively desensitized state that may be a result of constitutive phosphorylation of D1R by specific GRKs. The D1R has previously been shown to be constitutively phosphorylated and desensitized by overexpression of GRK-4 (Rankin et al., 2006) and caveolin has been shown to inhibit GRK activity (Carman et al., 1999). The disruption of these caveolin interactions at the level of the receptor or the kinase may release this tonic level of inhibition that results in constitutive phosphorylation and desensitization. Although this issue requires further study, previous reports have shown that agonist-dependent cAMP production by the $\beta_2$-adrenergic receptor in a sphingolipid-deficient (and hence, caveolae-deficient) cell line is enhanced only at higher agonist concentrations (Miura et al., 2001), consistent with the effects we observed with m$\beta$CD and overexpressed caveolin-1 P132L. This suggests that the lipid-enriched environment of morphological caveolae has additional effects on D1R-mediated signaling and that caveolae-dependent signaling is not strictly defined by an interaction with caveolin-1, per se. We unexpectedly determined that pretreatment with m$\beta$CD was found to enhance basal GTP$\gamma$S binding to $G_s$ without a parallel basal increase in cAMP production. Furthermore, although agonist stimulation did not change GTP$\gamma$S binding levels, cAMP production was significantly enhanced. The increase in basal GTP$\gamma$S binding upon caveolae disruption suggested that the inactive state of the receptor/G protein complex was constrained by its localization in caveolar domains. Indeed, caveolin-1 has been shown to have a high affinity for the inactive GDP-bound state of $G_s\alpha$, and it can inhibit its function by suppressing the rate of basal GDP/GTP exchange (Li et al., 1995). As a result, methyl-$\beta$-cyclodextrin mediated disruption of caveolae may release the inhibitory effect of caveolin-1 on $G_s\alpha$, thus facilitating GTP binding. The agonist-induced increase in cAMP, under caveolae-disrupted conditions, may be a result of an agonist-induced conformational reorganization of a pre-existing D1R-$G_s\alpha$ complex (Galés et al., 2006) that may facilitate opening of the $G_s\alpha$ interface to more efficiently interact with adenylyl cyclase. This conformational change may act in concert with the maximally activated G protein to enhance cAMP. These data suggest that caveolae have an inhibitory role on G protein activation and effector signaling by GPCRs specifically coupled to $G_s$ or $G_{i/o}$ (Rybin et al., 2000; Xu et al., 2006), which is in contrast to the facilitation of $G_q$-coupled receptor signaling by caveolar localization (Navratil et al., 2003; Bhatnagar et al., 2004). In previous studies, caveolin-2 was implicated in D1 receptor localization, and it was required for agonist-mediated cAMP production (Trivedi et al., 2004; Yu et al., 2004). These studies were performed in rat renal proximal tubule cells, which do not express caveolin-1, which is requisite for the formation of caveolae. Therefore, these specific cells do not form functional caveolae, suggesting that a distinct subset of lipid rafts mediate these effects and that different caveolin subtypes have unique roles in modulating D1 receptor signaling.

In summary, we have shown that caveolin-1 functionally interacts with the D1 dopamine receptor to modulate cAMP signaling and regulate receptor internalization. We demonstrate that this interaction is mediated by a specific caveolin binding motif in the receptor that has important implications in agonist-induced receptor sequestration. We have also provided evidence for the physiological occurrence of this interaction in rat brain, in which the D1 receptor has isoform selectivity for caveolin-1α. Taken together, these data suggest that important regulatory processes involving the D1 receptor may be influenced by its association in caveolar microdomains.


### Acknowledgments

We thank Tuan Nguyen for technical assistance and Drs. Bryan Roth and Jeffrey Benovic for providing the cMyc-caveolin-1 and GRK2-K220R constructs, respectively.


### References


Allen JA, Halverson-Tamboli RA, and Rasenick MM (2007) Lipid raft microdomains and neurotransmitter signalling. *Nat Rev Neurosci* **8**:128–140.

Bhatnagar A, Sheffler DJ, Kroeze WK, Compton-Toth B, and Roth BL (2004) Caveolin-1 interacts with 5-HT2A serotonin receptors and profoundly modulates the signaling of selected Gαq-coupled protein receptors. *J Biol Chem* **279**:34614–34623.

Bu J, Bruckner SR, Sengoku T, Geddes JW, and Estus S (2003) Glutamate regulates caveolin expression in rat hippocampal neurons. *J Neurosci Res* **72**:185–190.

Cameron PL, Ruffin JW, Bollag R, Rasmussen H, and Cameron RS (1997) Identification of caveolin and caveolin-related proteins in the brain. *J Neurosci* **17**:9520–9535.

Cao TT, Mays RW, and von Zastrow M (1998) Regulated endocytosis of G-protein-coupled receptors by a biochemically and functionally distinct subpopulation of clathrin-coated pits. *J Biol Chem* **273**:24592–24602.

Carman CV, Lisanti MP, and Benovic JL (1999) Regulation of G protein-coupled receptor kinases by caveolin. *J Biol Chem* **274**:8858–8864.

Chini B and Parenti M (2004) G-protein coupled receptors in lipid rafts and caveolae: how, when and why do they go there? *J Mol Endocrinol* **32**:325–338.

Couet J, Li S, Okamoto T, Ikezu T, and Lisanti MP (1997) Identification of peptide and protein ligands for the caveolin-scaffolding domain. Implications for the interaction of caveolin with caveolae-associated proteins. *J Biol Chem* **272**:6525–6533.

Dykstra ML, Cherukuri A, and Pierce SK (2001) Floating the raft hypothesis for immune receptors: access to rafts controls receptor signaling and trafficking. *Traffic* **2**:160–166.

Fujimoto T, Kogo H, Nomura R, and Une T (2000) Isoforms of caveolin-1 and caveolar structure. *J Cell Sci* **113**:3509–3517.

Gáborik Z, Szaszak M, Szidonya L, Balla B, Paku S, Catt KJ, Clark AJ, and Hunyady L (2001) β-Arrestin- and dynamin-dependent endocytosis of the AT1 angiotensin receptor. *Mol Pharmacol* **59**:239–247.

Galbiati F, Volonte D, Gil O, Zanazzi G, Salzer JL, Sargiacomo M, Scherer PE, Engelman JA, Schlegel A, Parenti M, et al. (1998) Expression of caveolin-1 and -2 in differentiating PC12 cells and dorsal root ganglion neurons: caveolin-2 is up-regulated in response to cell injury. *Proc Natl Acad Sci U S A* **95**:10257–10262.

Galés C, Van Durm JJ, Schaak S, Pontier S, Percherancier Y, Audet M, Paris H, and Bouvier M (2006) Probing the activation-promoted structural rearrangements in preassembled receptor-G protein complexes. *Nat Struct Mol Biol* **13**:778–786.

Head BP, Patel HH, Roth DM, Murray F, Swaney JS, Niesman IR, Farquhar MG, and Insel PA (2006) Microtubules and actin microfilaments regulate lipid raft/caveolae localization of adenylyl cyclase signaling components. *J Biol Chem* **281:**26391–26399.

Igarashi J and Michel T (2000) Agonist-modulated targeting of the EDG-1 receptor to plasmalemmal caveolae. eNOS activation by sphingosine 1-phosphate and the role of caveolin-1 in sphingolipid signal transduction. *J Biol Chem* **275:**32363–32370.

Lamey M, Thompson M, Varghese G, Chi H, Sawzdargo M, George SR, and O'Dowd BF (2002) Distinct residues in the carboxyl tail mediate agonist-induced desensitization and internalization of the human dopamine D1 receptor. *J Biol Chem* **277:**9415–9421.

Li S, Okamoto T, Chun M, Sargiacomo M, Casanova JE, Hansen SH, Nishimoto I, and Lisanti MP (1995) Evidence for a regulated interaction between heterotrimeric G proteins and caveolin. *J Biol Chem* **270:**15693–15701.

Mason JN, Kozell LB, and Neve KA (2002) Regulation of dopamine $D_1$ receptor trafficking by protein kinase A-dependent phosphorylation. *Mol Pharmacol* **61:**806–816.

McCabe JB and Berthiaume LG (2001) N-Terminal protein acylation confers localization to cholesterol, sphingolipid-enriched membranes but not to lipid rafts/caveolae. *Mol Biol Cell* **12:**3601–3617.

Miura Y, Hanada K, and Jones TL (2001) G(s) signaling is intact after disruption of lipid rafts. *Biochemistry* **40:**15418–15423.

Miyazaki I, Asanuma M, Diaz-Corrales FJ, Miyoshi K, and Ogawa N (2004) Direct evidence for expression of dopamine receptors in astrocytes from basal ganglia. *Brain Res* **1029:**120–123.

Navratil AM, Bliss SP, Berghorn KA, Haughian JM, Farmerie TA, Graham JK, Clay CM, and Roberson MS (2003) Constitutive localization of the gonadotropin-releasing hormone (GnRH) receptor to low density membrane microdomains is necessary for GnRH signaling to ERK. *J Biol Chem* **278:**31593–31602.

Nohe A, Keating E, Underhill TM, Knaus P, and Petersen NO (2005) Dynamics and interaction of caveolin-1 isoforms with BMP-receptors. *J Cell Sci* **118:**643–650.

Okamoto Y, Ninomiya H, Miwa S, and Masaki T (2000) Cholesterol oxidation switches the internalization pathway of endothelin receptor type A from caveolae to clathrin-coated pits in Chinese hamster ovary cells. *J Biol Chem* **275:**6439–6446.

Rajendran L and Simons K (2005) Lipid rafts and membrane dynamics. *J Cell Sci* **118:**1099–1102.

Rankin ML, Marinec PS, Cabrera DM, Wang Z, Jose PA, and Sibley DR (2006) The D1 dopamine receptor is constitutively phosphorylated by G protein-coupled receptor kinase 4. *Mol Pharmacol* **69:**759–769.

Rapacciuolo A, Suvarna S, Barki-Harrington L, Luttrell LM, Cong M, Lefkowitz RJ, and Rockman HA (2003) Protein kinase A and G protein-coupled receptor kinase phosphorylation mediates β-1 adrenergic receptor endocytosis through different pathways. *J Biol Chem* **278:**35403–35411.

Roseberry AG and Hosey MM (2001) Internalization of the M2 muscarinic acetylcholine receptor proceeds through an atypical pathway in HEK293 cells that is independent of clathrin and caveolae. *J Cell Sci* **114:**739–746.

Rybin VO, Xu X, Lisanti MP, and Steinberg SF (2000) Differential targeting of β-adrenergic receptor subtypes and adenylyl cyclase to cardiomyocyte caveolae. A mechanism to functionally regulate the cAMP signaling pathway. *J Biol Chem* **275:**41447–41457.

Schwencke C, Yamamoto M, Okumura S, Toya Y, Kim SJ, and Ishikawa Y (1999) Compartmentation of cyclic adenosine 3′,5′-monophosphate signaling in caveolae. *Mol Endocrinol* **13:**1061–1070.

Trivedi M, Narkar VA, Hussain T, and Lokhandwala MF (2004) Dopamine recruits D1A receptors to Na-K-ATPase-rich caveolar plasma membranes in rat renal proximal tubules. *Am J Physiol Renal Physiol* **287:**F921–F931.

Vickery RG and von Zastrow M (1999) Distinct dynamin-dependent and -independent mechanisms target structurally homologous dopamine receptors to different endocytic membranes. *J Cell Biol* **144:**31–43.

Vrecl M, Anderson L, Hanyaloglu A, McGregor AM, Groarke AD, Milligan G, Taylor PL, and Eidne KA (1998) Agonist-induced endocytosis and recycling of the gonadotropin-releasing hormone receptor: effect of beta-arrestin on internalization kinetics. *Mol Endocrinol* **12:**1818–1829.

Wang H, Haas M, Liang M, Cai T, Tian J, Li S, and Xie Z (2004) Ouabain assembles signaling cascades through the caveolar $Na^+/K^+$-ATPase. *J Biol Chem* **279:**17250–17259.

Williams TM and Lisanti MP (2004) The caveolin genes: from cell biology to medicine. *Ann Med* **36:**584–595.

Wyse BD, Prior IA, Qian H, Morrow IC, Nixon S, Muncke C, Kurzchalia TV, Thomas WG, Parton RG, and Hancock JF (2003) Caveolin interacts with the angiotensin II type 1 receptor during exocytic transport but not at the plasma membrane. *J Biol Chem* **278:**23738–23746.

Xu W, Yoon SI, Huang P, Wang Y, Chen C, Chong PL, and Liu-Chen LY (2006) Localization of the kappa opioid receptor in lipid rafts. *J Pharmacol Exp Ther* **317:**1295–1306.

Yamamoto M, Toya Y, Schwencke C, Lisanti MP, Myers MG Jr, and Ishikawa Y (1998) Caveolin is an activator of insulin receptor signaling. *J Biol Chem* **273:**26962–26968.

Yu P, Yang Z, Jones JE, Wang Z, Owens SA, Mueller SC, Felder RA, and Jose PA (2004) D1 dopamine receptor signaling involves caveolin-2 in HEK-293 cells. *Kidney Int* **66:**2167–2180.

Zanassi P, Paolillo M, Montecucco A, Avvedimento EV, and Schinelli S (1999) Pharmacological and molecular evidence for dopamine D(1) receptor expression by striatal astrocytes in culture. *J Neurosci Res* **58:**544–552.


**Address correspondence to:** Dr. Susan R. George, Department of Pharmacology, University of Toronto, Medical Sciences Bldg., Rm 4358, Toronto, ON, Canada M5S 1A8. E-mail: s.george@utoronto.ca